C-N/TiO$_2$ photocatalysts: Effect of co-doping on the catalytic performance under visible light

V. Trevisan [a], A. Olivo [a], F. Pinna [a], M. Signoretto [a,*], F. Vindigni [b], G. Cerrato [b], C.L. Bianchi [c]

[a] Departement of Molecular Sciences and Nanosystems, Ca'Foscari University Venice and Consortium INSTM, RU of Venice, Dorsoduro 2137, 30123, Venezia, Italy
[b] Departement of Chemistry & NIS Centre of Excellence and INSTM, RU Torino, University of Torino, via P. Giuria 7, 10125 Torino, Italy
[c] Departement of Chemistry, Milan University and INSTM Consortium, Via Golgi 19, 20133 Milan, Italy

A R T I C L E   I N F O

A B S T R A C T

Aim of this work is the synthesis of titanium-based photocatalysts co-doped with both C and N, exhibiting improved photocatalytic activity under visible light irradiation. The preparation of the catalysts consists of a two step process: during the first one, the synthesis of the catalyst doped with nitrogen has been carried out, whereas in the second step carbon has been introduced in different amounts.

The photocatalytic activity has been evaluated in the gas phase reaction of NOx abatement under visible light irradiation. The characterization has been carried out by N$_2$ physisorption, TPO (temperature programmed oxidation), DRS (diffuse reflectance spectroscopy) and XPS (X-ray Photoelectron Spectroscopy) in order to investigate both structural and physico-chemical features of the samples and their correlation with the catalytic activity. An effective promotion effect of the dopants has been observed; in particular, the synergic co-presence of both N and C produced a significant narrowing of the TiO$_2$ band gap with the consequent extension of the photocatalytic activity towards the visible part of the light spectrum.

© 2014 Elsevier B.V. All rights reserved.

1. Introduction

In recent years, to face the problem related to the increasing emissions of pollutants, the research has been focused on the development of efficient and reliable technologies for the abatement of hazardous substances released in the atmosphere. Heterogeneous photocatalysis is an effective way to reduce pollution that has attracted particular interest and has been extensively studied because of the advantages associated with it, among which:

i. the degradation reaction already occurs at low concentrations of pollutants and in "environmental benign" conditions
ii. it is economical, as it allows to exploit sunlight;
iii. it requires no toxic additives.

These interesting features have turned this technique to be the most investigated for both air and water purification. The photocatalytic process involves the adsorption of the reactants on the catalyst surface which, when irradiated by photons with an appropriate wavelength, produces active chemical species with strong oxidizing power. Among the various systems, titanium dioxide is one of most studied photocatalytic materials, owing its success to the considerable advantage associated with its use: high chemical stability, low cost and low toxicity [1–4].

However, its large band gap (approximately 3.2 eV) requires the use of UV light ($\lambda < 387$ nm), being the employment of the much larger visible part of solar light inhibited. Unfortunately the solar energy includes only the 3–5% [5–8] of ultraviolet radiation, consequently environmental applications of pure TiO$_2$ are limited. During the last years a lot of efforts have been directed toward the development of modified titania which would be photocatalytically active also under visible light irradiation (visible light covers >50% of the solar energy [9]). Among the various approaches proposed [10], the following are the main ones:

- the band gap reduction, obtained by using a photosensitizer which is excited by lower energy visible wavelengths and is able to transferring excited electrons or holes to the TiO$_2$ matrix [11];
- the control of the recombination rate of photogenerated electron–hole pairs, which occurs at either boundaries and/or defects;
- decreasing the particles size, the distance that charges need to travel to reach the surface reaction sites is reduced, thus the recombination probability decreases [12];

- the promotion of oxidation reactions and absorption of reactants on the catalyst surface, providing both right amount and type of active sites, by using porous materials that increase the specific surface area [13,14] or by using co-catalysts to introduce desirable active sites.

In particular, an increasing number of investigations have been focused on doped TiO_2: through the catalyst modification with appropriate elements, it is possible to promote the catalytic efficiency of plain TiO_2. A first type of doping concerns the introduction of transition metals, such as Fe, Cr, Ru, Mo, V and Rh [15–20]: these are likely to favor an increase of the catalytic activity by acting as charge traps for electron and/or holes of electrons, inducing both lowering the recombination rate and increasing catalysts life time. However, the obtained advantages are attenuated by some negative aspects related to the use of substances that can render thermally unstable the catalyst [21] and that are often toxic. In addition, high concentrations of metals are negative for the photocatalytic efficiency, by acting as electron–hole recombination sites [22].

The doping with non-metals, such as N, C, F, S, P [9,23–29], is an efficient alternative. Studies conducted on doping with N have brought to a considerable increase in the photocatalytic activity in the visible range [23,30]. Several investigations have shown that N promotes the overlap of the 2p oxygen orbitals with the 2p nitrogen orbitals, thus lowering the band gap of TiO_2 [31]. On the other hand, further studies propose the incorporation of N in the titania lattice (when added during the synthesis) as interstitial nitrogen by the creation of N–Ti–O and Ti–O–N bonds [32–36]. The generation of an intermediate energy state, between the conduction and the valence band, allows the promotion of electrons with light energy lower than in the undoped TiO_2. If N is therefore proposed as a good promoter activity for TiO_2, many studies have been devoted to the introduction of carbon [37–39]. The first studies regarding the introduction of C showed an appreciable increase of reaction rate in the electrolytic decomposition reaction of water into H_2 and O_2. As evidenced by Park et al. [40], carbon improves the photoactivity of titanium, but it is also likely to favor the stabilization of the anatase crystal phase and to promote the absorption of organic molecules on the catalyst surface.

In order to further increase the catalytic efficiency of TiO_2 in the visible region, the researchers have addressed their efforts towards the investigation of the co-doping with C and N: it has been found to be particularly successful [21]. These co-dopants, non-toxic and inexpensive, enhance the separation of the photoexcited electrons and holes, improving the photocatalytic efficiency: therefore, C and N co-doping increases the activity of pure TiO_2 under both visible and UV light irradiations [41]. Despite these numerous and interesting studies, many efforts are still needed to the optimization of an effective method which would allow the simultaneous introduction of dopants (C and N) during the synthesis step in order to maximize the subsequent catalytic activity.

The final goal of this work is then directed to both synthesis and characterization of stable TiO_2-based co-doped photocatalysts with improved performance under visible light irradiation. The catalytic performance will be evaluated in the gas phase reaction of NOx abatement.

2. Materials and methods

2.1. Synthesis

The following reagents were used as received: $TiOSO_4 \cdot xH_2SO_4 \cdot yH_2O$ (Aldrich), NH_3 (Riedel de Haen), succinic acid ($HOOC-CH_2CH_2-COOH$, Sigma–Aldrich).

The features and catalytic performances of the prepared catalysts were compared to those of the commercial Degussa P25 TiO_2 used as a standard reference material.

The N-TiO_2 samples were prepared by the precipitation method as previously reported [30]. Briefly, $TiOSO_4 \cdot xH_2SO_4 \cdot yH_2O$ was dissolved in distilled water at room temperature under vigorous stirring. A transparent solution was obtained and the pH was <1. $Ti(OH)_4$ precipitation was obtained by addition of a 9 M NH_4OH solution, used as N source. The pH was controlled during the base addiction and it was regulated until reaching the desired final value (7.0). The obtained suspension was magnetically stirred at 60 °C for 20 h. After this aging time, the solid was filtrated, washed with distilled water in order to remove $SO_4^=$ ions and dried in an oven at 110 °C over night. Then, the $Ti(OH)_4$ was crushed and pulverized and calcined for 4 h in an air flow at 300 °C in flowing air. The final samples were labeled N-TiO_2.

N-TiO_2 systems were subsequently doped with carbon by three different approaches using succinic acid as C precursor:

- Wet impregnation of $Ti(OH)_4$
- One-pot synthesis
- Wet impregnation of TiO_2

2.1.1. $Ti(OH)_4$ wet impregnation (WTH: wet impregnation on titanium hydroxide)

The $Ti(OH)_4$ powder was suspended in distilled water (25 wt% solids) and stirred at 60 °C. A variable amount of succinic acid, from 2 wt% to 12 wt% referred to the solid, was added and slowly stirred until the complete dissolution of the organic compound. The obtained suspension was gradually dried in vacuum to partially eliminate the solvent. Then it was put in an oven overnight at 110 °C [42].

2.1.2. One-pot synthesis (OT: one-pot titania)

This synthesis provides for the introduction of the carbon precursor by a one-step approach during the $Ti(OH)_4$ precipitation step. After the dissolution of the $TiOSO_4 \cdot xH_2SO_4 \cdot yH_2O$, various amounts of succinic acid (0.5–2 wt%) were added to the solution in order to obtain the desired final content of C. The C-$Ti(OH)_4$ precipitation was performed by addition of 9 M NH_4OH solution. The obtained suspension was aged at 60 °C for 20 h, filtered, washed with distilled water in order to remove $SO_4^=$ ions and dried in an oven at 110 °C over night.

2.1.3. Wet impregnation TiO_2 (WT: wet impregnation on titanium oxide)

N-TiO_2 samples were doped with the suitable amount of succinic acid, from 0.5 wt% to 5 wt%, by following the procedure reported for the WTH systems (paragraph 1).

The calcination temperature of the doped systems was selected after TPO analysis of the dried samples. It was found that the oxidation of carbonaceous species in the samples starts at 250 °C [42]. In order to avoid the complete elimination of the inserted dopants, we chose to treat all the synthesized systems at 250 °C for 2 h in flowing air.

The calcined samples were labeled as follows:
WTHx = W: wet – **TH**: titanium hydroxide – **x**: % ac. succ.; **OTx = O**: one pot – **T**: titanium oxide – **x**: % ac. succ.; **WTx = W**: wet – **T**: titanium oxide – **x**: % ac. succ.

2.2. Characterization

Surface area and pore volume were obtained from N_2 adsorption–desorption isotherms at −196 °C using a MICROMERITICS ASAP 2000 Analyser. Prior to N_2 physisorption experiments, all samples were outgassed at 200 °C for 2 h. Mesopore volume was
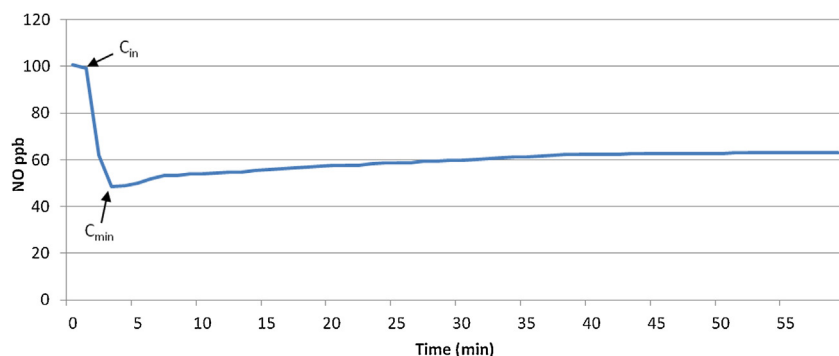
Fig. 1. Typical concentration profile of NO.

measured as the adsorbed amount of N_2 after capillary condensation. Surface area was calculated using the standard BET [43] equation method and pore size distribution was elaborated using the BJH method applied to the isotherms adsorption branch [44].

X-ray diffraction (XRD) patterns of the samples were collected by means of a Bruker D8 Advance powder diffractometer equipped with a sealed X-ray tube (copper anode; operating conditions, 40 kV and 40 mA) and a Si(Li) solid state detector (Sol-X) set to discriminate the Cu Kα radiation. Measuring conditions were 40 kV × 40 mA. Apertures of divergence, receiving and detector slits were 2.0 mm, 2.0 mm, and 0.2 mm respectively. Data scans were performed in the 2θ range 5–75° with 0.02° stepsize and counting times of 3 s/step.

TPO (temperature programmed oxidation) experiments were carried out in a lab-made equipment: samples (50 mg) were heated at 10 °C/min from 25 °C to 700 °C in a 5% O_2/He oxidative mixture (40 mL/min STP). The effluent gases were analyzed by a Gow-Mac TCD detector using a basic trap with soda lime to stop CO_2 and a magnesium perchlorate trap to stop H_2O.

The amount of nitrogen and carbon were obtained by elemental analyses with a Carlo Erba CNS Autoanalyser, mod. NA 1500. All analyses were replicated 2–3 times and the precision was >95%.

The band gap was obtained by Diffused reflectance spectroscopy (DRS) employing a Varian spectrophotometer (Cary 5000), equipped with an accessory for the measurement of diffuse reflectance. The incident beam was collimated and the reflected light was analyzed by an integrating sphere Spectralon®. The white reference was obtained by a teflon disc.

XPS surface characterization were performed by means of an XPS instrument (M-Probe – SSI) equipped with a monochromatic Al Kα source (1486.6 eV) with a spot size of 200 × 750 μm and a pass energy of 25 eV, providing a resolution for 0.74 eV. For all the samples, the C1s peak level was taken as internal reference at 284.6 eV. The accuracy of the reported binding energies (BE) can be estimated to be ±0.2 eV. The quantitative data were also accurately checked and reproduced several times and the percentages error is estimated to be ±1%. Survey spectra were recorded with 256 scans and 1 eV/pt to reduce the ground noise and allow the detection of nitrogen eventually present at the sample surface.

SEM analyses were carried out with a Hitachi TM3000 operating under high vacuum at an accelerating voltage of 15 keV. All the samples were coated with gold (Cressington 108 auto sputter coater) before the SEM characterization.

2.3. Photocatalytic test

The photocatalytic activity of the samples was evaluated in the NO*x* oxidation reaction using an experimental apparatus as previously reported in [45]. The gas phase reaction was carried out in a fixed-bed reactor at atmospheric pressure and room temperature by feeding of the reaction mixture (1000 mL/min NO/air, 100 ppb of NO). In a typical experiment, the catalysts (50 mg) were previously pressed, ground and sieved to 50–70 mesh (0.2–0.3 mm), and then were introduced into a 2 mm internal diameter microreactor irradiated with a visible lamp (fluorescent energy saver lamp, Philips WW 827, 14 W, 7.4 W/m²). The catalytic efficiency is expressed in terms of conversion of NO, calculated with the following equation [23,46]:

$$\text{conversion}\% = \frac{C_{in} - C_{min}}{C_{in}} \times 100$$

where C_{in} is the initial concentration of NO and C_{min} is the minimal concentration of NO.

The catalytic conversion reported was determinated as the average of three independent analyses.

Before starting the photooxidation reaction, the reactor was purged and saturated with pure air.

NO concentration was monitored in continuous and a typical profile of such concentration as a function time has been reported in Fig. 1 as representative plot [47–49].

As it can be observed, NO concentration reaches a minimum value followed by a slow and continuous deactivation process after the adsorption of NO_3 on the catalytic active sites [45]. Based on the above considerations, the minimum value of the concentration of NO was considered as key parameter for the evaluation of the catalytic performances.

3. Results and discussion

The principal goal of the work is the optimization of a reliable and effective approach for the synthesis of TiO_2 photocatalysts with improved activity in the abatement of NO*x* under visible light irradiation. In a previous study [30] we have already verified the positive influence of N doping on the photocatalytic performance of TiO_2 under visible light: in the present research in order to extend
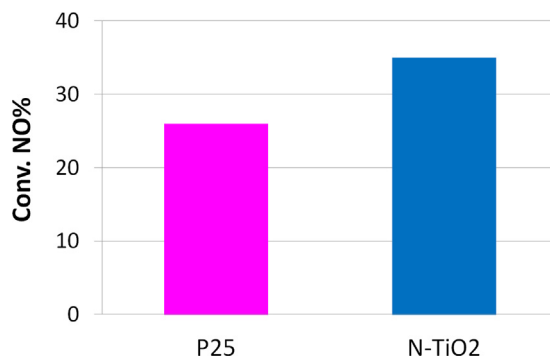

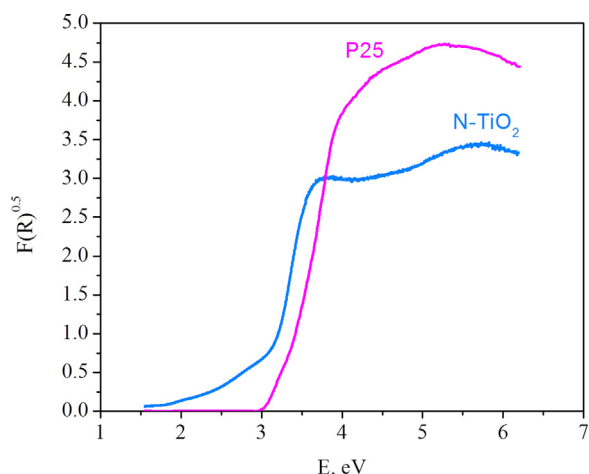**Fig. 2.** NO conversion for a N-TiO$_2$ system and for the TiO$_2$ P25.

Fig. 3. Diffuse reflectance spectra.

Fig. 4. NO conversion for WTH-*x* and N-TiO$_2$ system.

the investigation on these systems, the N-TiO$_2$ catalysts have been reconsidered as starting point. As far as NO conversions for a N-TiO$_2$ sample and for a commercial TiO$_2$ P25 (Evonik), used as reference, the results are reported in Fig. 2.
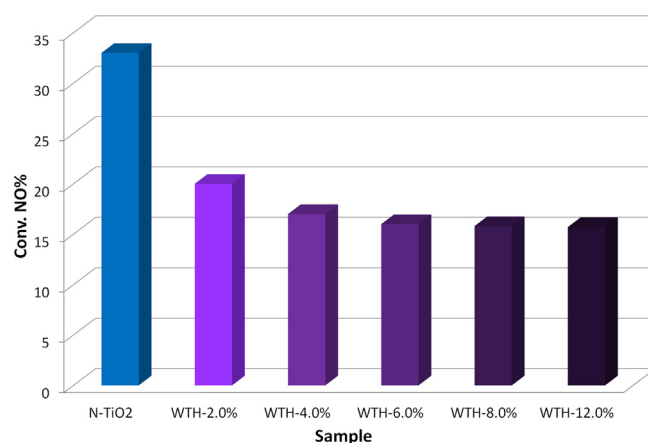
N-TiO$_2$ reveals an improved photoactivity. The investigation of the factors that can affect the efficiency under visible light irradiation led to look for confirmation in the evaluation of the band gap by Diffuse Reflectance Spectroscopy (DRS) analysis: see Fig. 3.

The energy band gap value is calculated extrapolating the intercept of the tangent to the curve on the *x*-axis. The band gap for the commercial P25 sample turns out to be approximately 3.2 eV, whereas it is 2.9 eV in the case of N-TiO$_2$. The narrowing of the band gap may indicate that the precipitation of the Ti precursor with ammonia can facilitate the introduction of nitrogen in the titanium dioxide lattice with a positive influence on the catalytic performance of the doped sample. Probably, nitrogen replaces some of the oxygen atoms, creating vacancies and generating a sub-layer energy between the valence band and the conduction band, leading to the activation of the catalyst even under visible light irradiation [22]. In the present case the narrowing of the band gap can be the result of electronic transitions from intra-gap localized levels, located above the valence band, up to the conduction band.

In order to further increase the catalytic performance, a series of co-doped TiO$_2$ systems have been also synthesized by introducing carbon as second dopant element, employing succinic acid as organic source as previously reported [42]. These samples have been synthesized as reported in the experimental section (WTH) with an increasing amount of succinic acid (from 2 to 12 wt%), keeping unchanged the N percentage.

The best catalytic performance is exhibited by the N-TiO$_2$ sample, whereas a reduction of the photocatalytic activity is detected for all the co-doped systems (see Fig. 4).

This unexpected result can be explained by the effective amount of C and N present in the WTH samples: see Table 1. In fact, in all the co-doped catalysts the N percentage is almost negligible and the

Table 1
Elemental analyses for WTH-*x* and N-TiO$_2$ system.

Sample	%N	%C
WTH-12.0%	0.03	2.90
WTH-8.0%	0.03	2.05
WTH-6.0%	0.06	1.52
WTH-4.0%	0.04	1.07
WTH-2.0%	0.03	0.58
N-TiO$_2$	0.35	0.01

procedure adopted for the C introduction is likely to be the cause of the nitrogen loss.

It seems evident that it is necessary to improve the synthetic approach in order to maintain nitrogen in the proper amount: to do so, several methodologies of dopants introduction were then investigated, with the aim of identifying the best approach to obtain a final co-doped catalyst in which the co-presence of both C and N is ensured, highly performing in the NO*x* abatement under visible light.

To this end a proper amount of carbon was introduced by a one-pot synthetic approach during either the Ti(OH)$_4$ precipitation (OT) or by wet impregnation on TiO$_2$ (WT) with 2% succinic acid.

The TPO profiles for the three co-doped samples and for the reference N-TiO$_2$ are reported in Fig. 5.

The total absence of peaks related to oxygen consumption for the TiO$_2$ sample prepared by a one pot approach (curve A) is evident: succinic acid, being a very soluble compound, is likely to be eliminated during the washing procedure necessary to remove the counter-ions (sulfates) deriving from the titania precursor. On the other hand, the TPO profile of the WTH system (curve B) exhibits a well-defined peak due to the carbon precursor degradation at about 300–350 °C, whereas no peaks ascribable to N oxidation were detected, in agreement with the data reported in Table 1. Moreover, two well-defined peaks are observed for the WT system (see curve C): they are related to the presence of oxidizable species that can to be assigned to oxidation of carbon (at 300 °C) and nitrogen (at
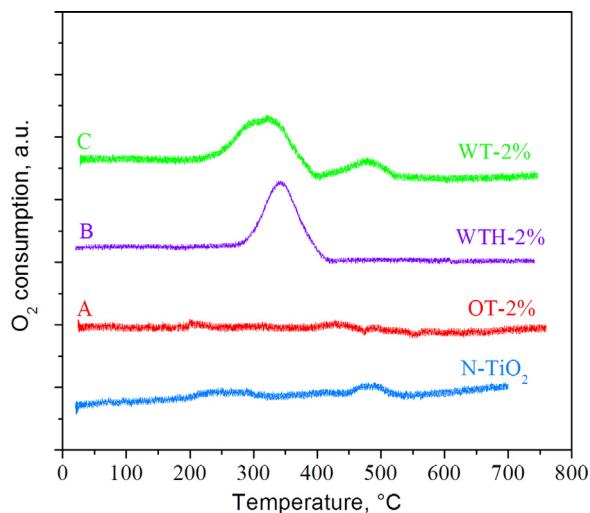

Fig. 5. TPO analyses for the three co-doped samples and N-TiO$_2$.
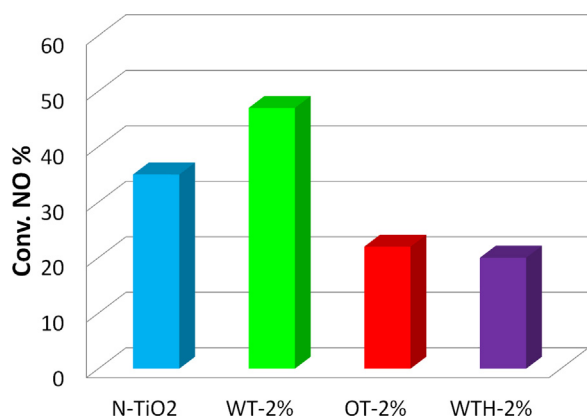
Fig. 6. NO conversion for WTH-2.0%, OT-2.0%, WT-2.0% and N-TiO$_2$ systems.

Fig. 8. TPO analyses for the various WT samples prepared with different amounts of carbon.

450 °C) species, as confirmed by quadrupole mass analyses. It can be then preliminary concluded that the WT sample, synthesized by wet impregnation on the parent N-TiO$_2$, represents a real C,N co-doped system.

The catalytic results obtained for the NO photoxidation with visible light for the three different co-doped samples are reported in Fig. 6, in which the N-TiO$_2$ sample has been taken as a reference.

A decreasing trend in the photocatalytic activity is evident as a function of the preparation route: the sample prepared by wet impregnation on N-TiO$_2$ (see for instance the green histogram for WT-2.0%) reveals a good NO conversion (∼47%), being also more active than the N-TiO$_2$ sample (see the blue histogram, NO conversion ∼35%). On the contrary, when the carbon introduction is carried out either in the precipitation step (see the red histogram, OT-2.0% sample) and by impregnation of the Ti(OH)$_4$ (see the violet histogram, WTH-2.0% sample), the photocatalytic conversion exhibit the worst results (22–20%).

The co-presence of both C and N in WT-2.0% can then explain the best catalytic performance observed for WT-2.0% sample.

Furthermore, the introduction of carbon has almost no effect on the crystalline form. If we compare the XRD patterns relative to WT-2.0% and N-TiO$_2$ samples, reported in Fig. 7, it can be noted that only the anatase phase has been detected. Therefore, the carbon introduction does not modify the crystal phase of TiO$_2$ to any extent.
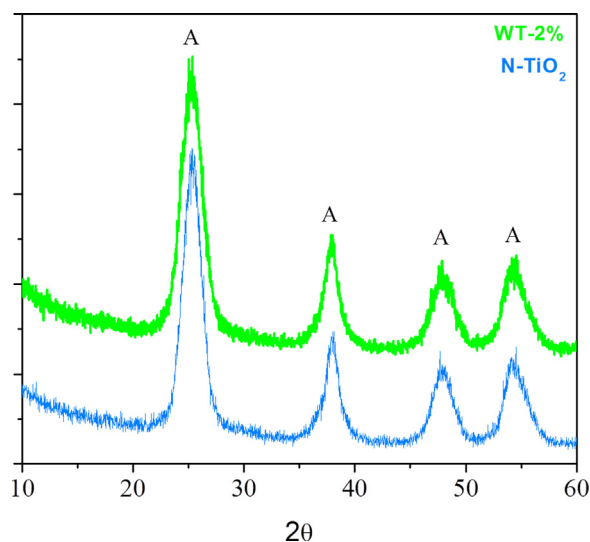
On the basis of these experimental evidences, the research has been directed only toward this most promising system (WT-x): the effect of the amount of succinic acid (in the 0.5–5.0 wt% range) on both physico-chemical features of titania and on its catalytic performance has been investigated in detail.

Also in this case, in order to verify the presence of both N and C dopants in each sample, we have performed the TPO analysis on all C,N-TiO$_2$ obtained by the WT preparation route (see Fig. 8).

The TPO profiles of all the co-doped systems exhibit the two peaks previously described and ascribable to the presence of both C and N species. The former started at 250 °C, exhibited a maximum at about 300 °C and it is associated with the oxidation of carbon; the latter is located at 450 °C and is related to nitrogen species. The intensity of the first peak increases proportionally to the amount of the organic source and, moreover, it is evident a decrease of the starting oxidation temperature of these compounds as far as the amount of succinic acid introduced is increased. In fact, a larger amount of organic precursor brings about the formation of carbonaceous species on the outer surface of the catalyst, exhibiting a faster/easier oxidation. The second peak is similar in all TPO curves, and it indicates that almost the same amount of N is present in all the calcined photocatalysts (0.35 wt%, as confirmed by elemental analyses).

The catalytic performance of these systems has been then evaluated in the photocatalytic oxidation of NO under visible light irradiation. For all the samples the catalytic conversion reported was determinated as described in the experimental section as the average of three independent analyses. From each NO concentration profile, we have calculated the initial rate of reaction (Δppb NO/min) and we have observed an increment from 12 ppb/min for the N-TiO$_2$ sample to 14 ppb/min for WT-5.0% and finally 20 ppb/min for WT-0.5%. This trend was the same observed for the average catalytic conversion reported in Fig. 9.

All the samples exhibit a very good NOx conversion with a maximum for the lowest concentration of C precursor (0.5 wt%). Moreover, a significant increase of activity under visible light irradiation is observed for all WT-x samples, if compared to both standard commercial P25 and plain doped N-TiO$_2$ system. These results allow us to confirm the efficiency of the synthetic approach (TiO$_2$ wet impregnation), the validity of the co-doping with N and C and the synergistic interaction between these dopants.

Concerning the co-doped WT-x systems, their photocatalytic activity seems to be inversely proportional to the amount of introduced carbon, and in order to better understand this activity trend, we have performed a thorough physico-chemical characterization.

Fig. 7. XRD (A: anatase) for WT-2.0% (green line) and N-TiO$_2$ (blue line).(For interpretation of the references to color in this figure legend, the reader is referred to the web version of the article.)
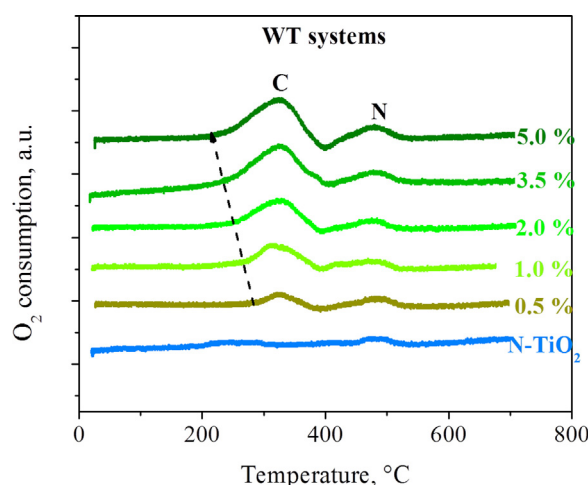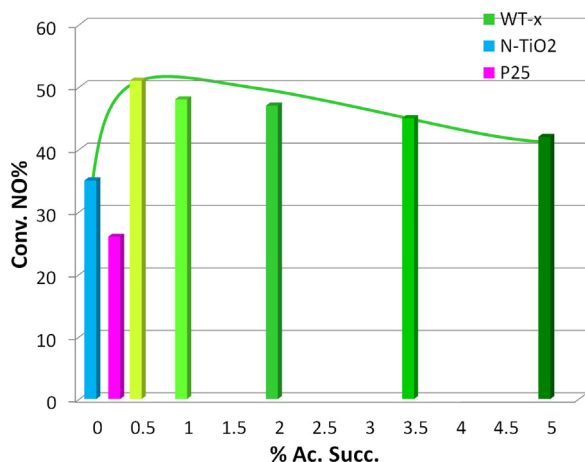
Fig. 9. Catalytic results obtained for WT-*x* catalysts (green histograms), including a N-TiO$_2$ sample (blue histogram) and for the reference P25 (pink histogram).(For interpretation of the references to color in this figure legend, the reader is referred to the web version of the article.)

Table 2
BET surface area for all the WT-*x* samples.

Sample	Surface area (m^2/g)
N-TiO$_2$	200
WT-0.5%	198
WT-1.0%	186
WT-2.0%	182
WT-3.5%	195
WT-5.0%	193

Table 3
Band gap values for the WT-0.5% and WT-5.0% systems, N-TiO$_2$ and for a P25 reference standard.

Sample	Apparent band gap energy(eV)
P25	3.20
N-TiO$_2$	2.88
WT-5.0%	2.75
WT-0.5%	2.63

The introduction of C and its amount have almost no effect on the structural features of the final samples, in particular preserving the high specific surface area (see Table 2), the average pore diameter (4 nm in all samples), the pore volume (0.16–0.22 cm^3/g). Moreover all the samples exhibited only the anatase polymorph and the average crystallites diameter calculated by XRD using Rietveld elaboration was similar for all samples (∼3.3 nm).

The morphological features of the various TiO$_2$-based materials have been investigated by means of SEM microscopy: see Fig. 10. All materials exhibit large aggregates (average dimensions: up to 100 μm) of particles made up of much smaller crystallites.

No relevant difference can be evidenced among the various samples even after inspection at higher magnification, see Fig. 11.

On the basis of all the data obtained so far, it is evident that the morphological and structural properties are then insufficient to explain the differences in photoactivity.

We decided to investigate the electronic properties of the all the samples of interest by Diffuse Reflectance Spectroscopy (DRS): a detail of the apparent band gap energy has been reported in Fig. 12, as well as the apparent band gap values in Table 3.

In the detail of DRS spectra we can observe a sharp absorption at about 3.2 eV (400 nm) relative to the P25 commercial sample. If we compare the energy values of either doped and/or co-doped samples, it is evident that these are extended to the visible region in the 2.3–3.1 eV (520–400 nm) range. This effect is more evident for all the WT-*x* systems, in which the absorption edge exhibits an
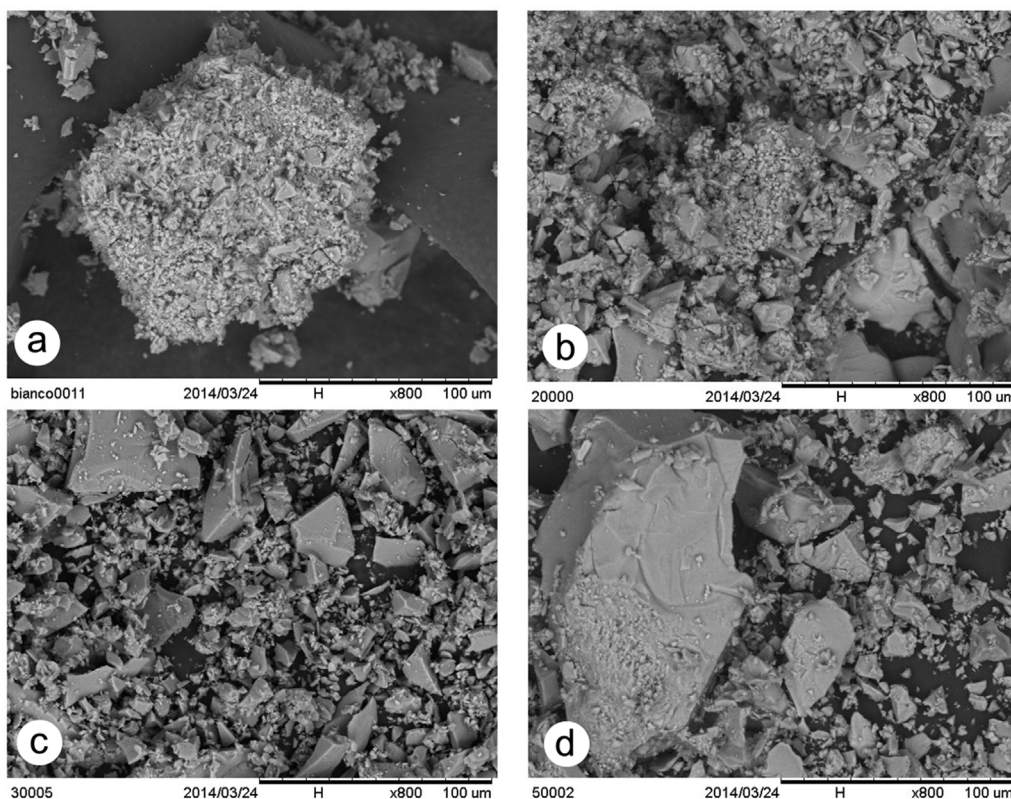

Fig. 10. Low magnification images.
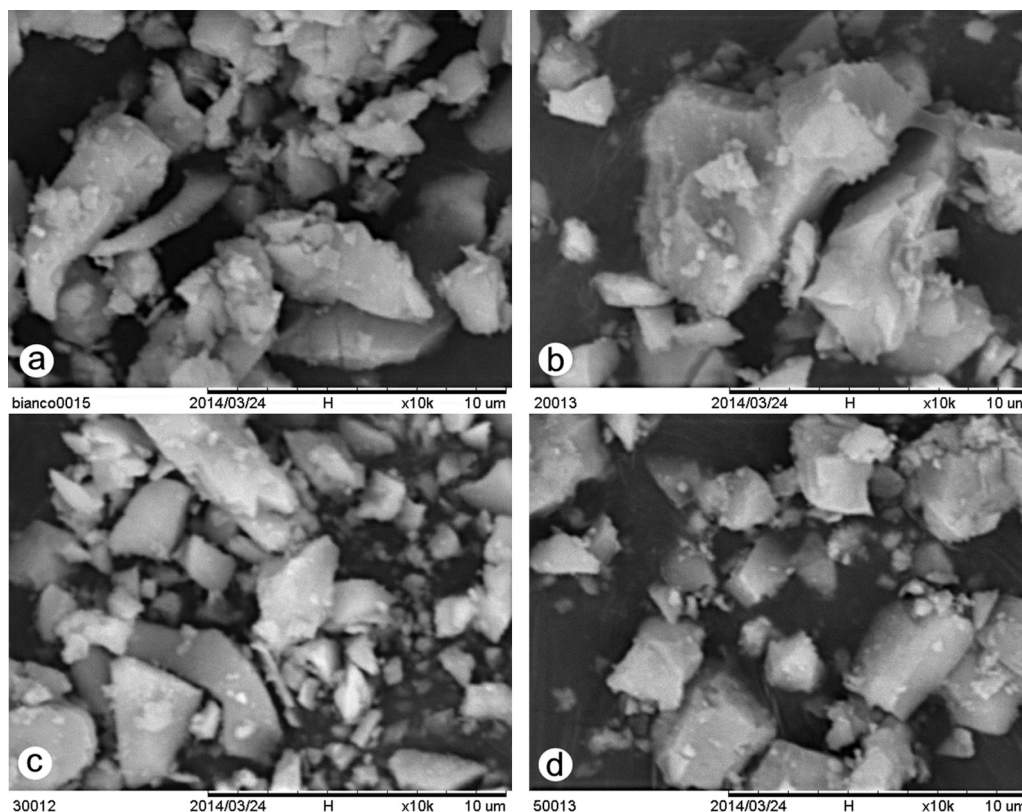Section a: N-TiO$_2$; section b: WT-2.0%; section c: WT-3.5%; section d: WT-5.0%.

Fig. 11. High magnification images.
Section a: N-TiO$_2$; section b: WT-2.0%; section c: WT-3.5%; section d: WT-5.0%.

evident red-shift, indicating a possible synergistic effect of the two dopants [50].

As reported in Table 3, we can observe a first considerable reduction of the apparent band gap energy in the N-TiO$_2$ sample with respect to the P25 reference, due to N-doping, and a further decrease of the apparent band gap in the co-doped sample according to the results reported by Konstantinova et al. [38]. In fact, experimental and theoretical studies indicate that the addition of carbon generates localized energy levels (or surface states) just above the valence band. The carbon-doped titania thus exhibits

an increased activity under visible light irradiation [38], due to the presence of these intra-band gap states.

The band gap energy of these samples can be tentatively correlated with the photoactivity data, as reported in Fig. 13.

The trend confirms the close correlation between the apparent band gap and the catalytic activity under visible light irradiation. All the co-doped systems reveal a lower apparent band gap than the P25 sample, that in fact exhibits the worst performance. In particular, it can be observed that the most active sample (WT-0.5% in which we find 0.35 wt% N and 0.5 wt% succinic acid) exhibits the lowest band gap (2.63 eV). The co-presence of N and C seems to cause a narrowing of the band gap of TiO$_2$ with the consequent extension of its activity to the visible spectrum.

This positive effects on the photoactivity of titania have been recently confirmed by an in-depth computational work on the electronic effects induced by non-metal doping on the electronic structure of TiO$_2$ [51]: boron, carbon, nitrogen, fluorine and iodine
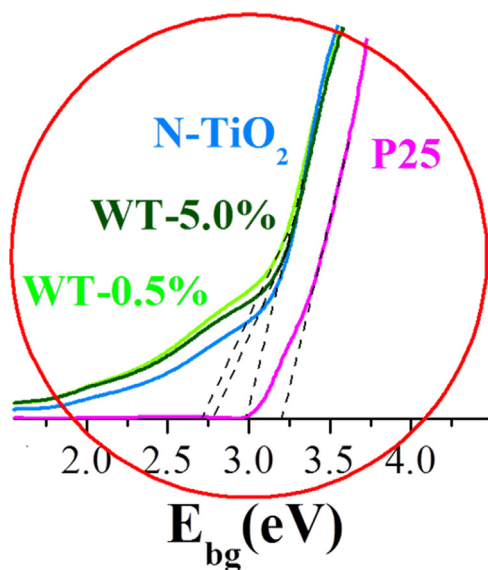

Fig. 12. Detail of the DRS spectra as a function of band gap energy for WT-0.5% and WT-5.0% systems, N-TiO$_2$ and for a P25 reference standard.
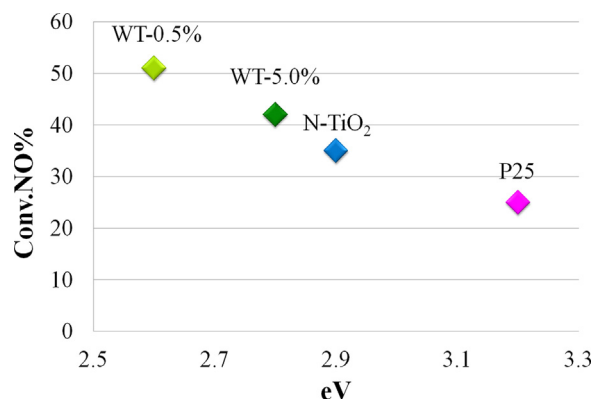

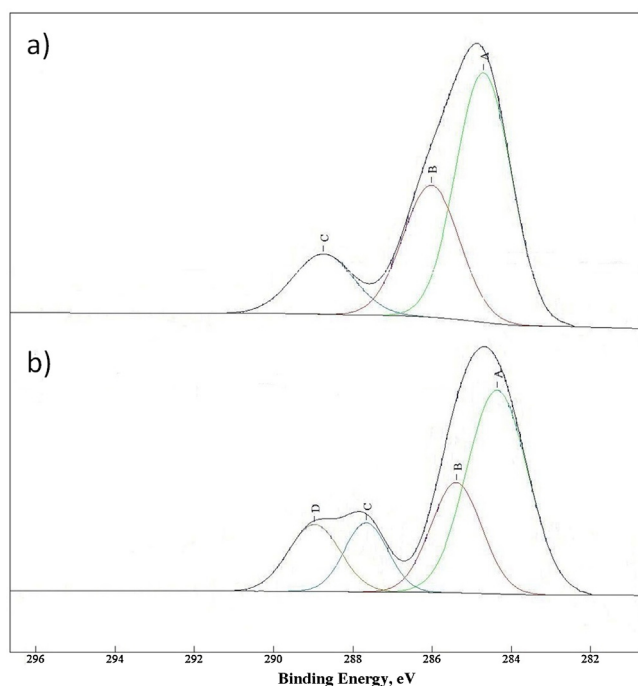**Fig. 13.** Correlation between the band gap and the NO conversion.

Fig. 14. C(1s) spectra for (a) WT-0.5% and (b) WT-5.0% systems.

Table 4
Surface composition detected by XPS for WT-0.5% and WT-5.0% samples.

	%C	%O	%Ti	%N
WT-0.5%	21.1	57.1	21.4	0.4
WT-5.0%	18.1	56.9	24.6	0.4

are the most investigated. The introduction of N dopant in the TiO$_2$ lattice may affect the band edge and its role is very clear. In this case, the dopant can either substitute oxygen in the titanium dioxide lattice or occupy interstitial sites. In both cases a red shift in the light absorption of titania is observed and can be due to a decrease in the apparent band gap energy. For all the other dopants the effect on the catalytic activity and the interaction between each other is not so well-defined. In particular, the effective mechanism of carbon doping on the photoactivity enhancement also remains not fully understood. The difficulty depends mainly on the different synthetic routes: it is widely accepted that a red shift occurs, but there are many different interpretations about (i) the role played by the carbon atoms and (ii) the way by which the visible light is absorbed. The formation of Ti–C, C–Ti–O, C–O and C–C bonds and of oxygen vacancies as well, the creation of C 2p mid-gap states [52,53] and of mid-gap states due to the mixing of C 2p and O 2p orbitals, have been hypothesized and positive effects are only verified in the case of co-doped systems.

In order to shed some light onto the surface chemical composition of the various doped TiO$_2$ materials, High-Resolution XPS spectroscopy has been resorted to. As for what concerns in the region of carbon, the XPS spectra corresponding to WT-0.5% and WT-5.0% systems are reported in Fig. 14.

The WT-0.5% sample (see set a) exhibits three peaks in this spectral range, that can be respectively ascribed to the following species: (i) C–H (component A = 284.6 eV), (ii) C–OH and C–N (component B = 285.9 eV) and (iii) C=O (component C = 288.6 eV).

Unfortunately, the overlap of the peaks corresponding to both C–OH and C–N bonds allows no distinction between the two ones.

As for the C=O component, Ren et al. [54] observed that it corresponds to a carbonate species present in C-doped titania systems and concluded that carbon may substitute some of the lattice titanium atoms forming a Ti–O–C structure.

The sample WT-5.0% (see set b) exhibits an additional peak located at 287.6 eV (component C), most likely due to the presence of an oxidized carbon type. According to the literature [55,56], both substitution with carbon of the lattice oxygen in the titania and the formation of carbonates species in titania lead to the narrowing of

the band gap in the final obtained carbon-doped system, and this is the case of the WT-5.0% sample.

Moreover, it has been reported [57,58] that high doping levels cannot be achieved because of the high formation energy due to too different ionic charge and radius between the doping ions and the hosting ones. High amount of carbon leads to an increased absorption in the visible region, but it simultaneously promotes the recombination of the charge carriers. A synergistic effect due to the co-presence of two (or more) complementary dopants seems to solve this problem [57–60], leading to an improved photoactivity of TiO$_2$ in the visible light region, if compared to either pure or single-doped TiO$_2$.

As for the XPS spectra collected in the region of titanium, in the case of the WT-0.5% sample the typical peaks of 2p$_{3/2}$ and 2p$_{1/2}$ orbitals (458.5 and 464.2 eV), respectively, are evident confirming the presence of only Ti(IV) species. Also in the case of the WT-5.0% sample, the spectra exhibits the same two peaks for Ti, with a shift of about 0.35 eV towards lower energies (458.1 and 463.9 eV, respectively, for Ti 2p$_{3/2}$ and Ti 2p$_{1/2}$ orbitals).

This effect can be attributed to a higher content of titanium (from 21.4 to 24.6% at., see Table 4) for the WT-5.0 sample and, consequently, to a lower influence of carbon on the electronic structure.

In fact, the higher the content of carbon, the more electropositive the character of titanium, so we can observe that for this sample the main peaks are located at higher energies. This evidence could also explain the photoactivity trend of the co-doped catalysts.

Even if the XPS spectra have been also collected in the region of N 1s, no information can be obtained from the spectra themselves, as they exhibit a very high signal-to-noise ratio, in which the XPS component due to N species cannot be singled out to obtain a reliable fitting: this might be due to the very low concentration of this element in both the samples (0.4% at.).

4. Conclusions

We have optimized a relatively easy and effective method for the preparation of active co-doped photocatalysts. The synergic presence of C and N greatly improves the photocatalytic activity (51%) that is higher than that of both a commercial standard (25%) and of a single-doped N-TiO$_2$ systems (35%), acting on the decreasing of the apparent band gap energy which is one of the most effective limitations related to this type of catalysts.

This action makes possible the exploitation of such a catalyst in the presence of sunlight, making the process more environmentally friendly and expanding the field of applications of TiO$_2$ materials to the efficient use in the open air.

Appendix A. Supplementary data

Supplementary data associated with this article can be found, in the online version, at http://dx.doi.org/10.1016/j.apcatb.2014.05.015.

References

[1] J. Orth-Gerber, et al., U.S Patent, US 20,050,226,761 (2005).
[2] T. Ohno, K. Sarukawa, K. Tokieda, M. Matsumura, J. Catal. 203 (2001) 82–86.
[3] R. Zhang, Y. Bai, B. Zhang, L. Chen, B. Yan, J. Hazard. Mater. 211–212 (2012) 404–413.
[4] S. Hackenberg, G. Friehs, K. Froelich, C. Ginzkey, C. Koehler, A. Scherzed, M. Urghartz, R. Hagen, N. Kleinsasser, Toxicol. Lett. 195 (2010) 9–14.
[5] K.M. Parida, B. Naik, J. Colloid Interf. Sci. 333 (2009) 269–276.
[6] Y. Yin, W. Zhang, S. Chen, S. Yu, Mater. Chem. Phys. 113 (2009) 982–985.
[7] J. Liu, W. Qin, S. Zuo, Y. Yu, Z. Hao, J. Hazard. Mater. 163 (2009) 273–278.
[8] Y. Cong, J. Zhang, F. Cheng, M. Anpo, J. Phys. Chem. 111 (2007) 6976–6982.
[9] C.L. Bianchi, G. Cappelletti, S. Ardizzone, S. Gialanella, A. Naldoni, C. Oliva, C. Pirola, Catal. Today 144 (2009) 31–36.
[10] R. Leary, A. Westwood, Carbon 49 (2001) 741–772.
[11] M. Ni, M.K.H. Leung, D.Y.C. Leung, K. Sumathy, Renewable Sustainable Energy Rev. 11 (2007) 401–425.
[12] A. Kudo, Y. Miseki, Chem. Soc. Rev. 38 (2009) 253–278.
[13] A.Z. Moshfegh, J. Phys. D: Appl. Phys. 42 (2009) 233001–233031.
[14] V. Chhabra, V. Pillai, B.K. Mishra, A. Morrone, D.O. Shah, Langmuir 11 (1995) 3307–3311.
[15] J. Li, J. Xu, W.L. Dai, H. Li, K. Fan, Appl. Catal. B: Environ. 85 (2009) 162–170.
[16] J.M. Pan, T.E. Madey, J. Vac. Sci. Technol. A 11 (1993) 1667–1674.
[17] G.A. Rizzi, M. Scambi, A. Magrin, G. Granozzi, Surf. Sci. 30 (2000) 454–456.
[18] S. Petigny, B. Domenichini, H. Mostefa-Sba, E. Lesniewska, A. Steinburnn, S. Bourgeois, Appl. Surf. Sci. 142 (1999) 114–119.
[19] J. Biener, M. Baumer, R. Madix, Surf. Sci. 450 (2000) 12–26.
[20] L. Yue, W. Hai-Qiang, W. Zhong-Biao, J. Environ. Sci. 19 (2007) 1505–1509.
[21] D. Chen, Z. Jiang, J. Geng, Q. Wang, D. Yang, Ind. Eng. Chem. Res. 46 (2007) 2741–2746.
[22] R. Jaiswal, N. Patel, D.C. Kothari, A. Miotello, Appl. Catal. B: Environ. 126 (2012) 47–54.
[23] N. Pernicone, F. Pinna, V. Trevisan, L. Cassar, G.L. Guerrini, L. Bottalico, Int. Patent, WO2011/045031 A1.
[24] Y. Nosaka, M. Matsushita, J. Nishino, A.Y. Nosaka, Sci. Technol. Adv. Mat. 6 (2005) 143–148.
[25] S.Y. Treschev, P.W. Chou, Y.H. Tseng, J.B. Wang, E.V. Perevedentseva, C.L. Cheng, Appl. Catal. B: Environ. 79 (2008) 8–16.
[26] Y. Yu, H.H. Wu, B.L. Zhu, S.R. Wang, W.P. Huang, S.H. Wu, S.M. Zhang, Catal. Lett. 121 (2008) 165–171.
[27] M. Hamadanian, A. Reisi-Vanani, A. Majedi, Mater. Chem. Phys. 116 (2009) 376–382.
[28] G. Colon, M.C. Hidalgo, J.A. Navio, A. Kubacka, M. Fernandez-Garcia, Appl. Catal. B: Environ. 90 (2009) 633–641.
[29] R. Asapu, V. Manohar Palla, B. Wang, Z. Guo, R. Sadu, D.H. Chen, J. Photochem. Photobiol. A 225 (2011) 81–87.
[30] V. Trevisan, M. Signoretto, F. Pinna, G. Cruciani, G. Cerrato, Chem. Today 30 (2012) 25–28.
[31] R. Asahi, T. Morikawa, T. Ohwaki, K. Aoki, Y. Taga, Science 293 (2001) 269–271.
[32] K.M. Parida, B. Naik, J. Colloid Interface Sci. 333 (2009) 269–276.
[33] H. Irie, Y. Watanabe, K. Hashimoto, J. Phys. Chem. B 107 (2003) 5483–5486.
[34] A. Kachina, E. Puzenat, S. Ould-Chikh, C. Geantet, P. Delichere, P. Afanasiev, Chem. Mater. 24 (2012) 636–642.
[35] M. Ceotto, L. Lo Presti, G. Cappelletti, D. Meroni, F. Spadavecchia, R. Zecca, M. Leoni, P. Scardi, C.L. Bianchi, S. Ardizzone, J. Phys. Chem. C 116 (2012) 1764–1771.
[36] N. Serpone, A.V. Emeline, J. Phys. Chem. Lett. 3 (2012) 673–677.
[37] X. Wang, S. Meng, X. Zhang, H. Wang, W. Zhong, Q. Du, Chem. Phys. Lett. 444 (2007) 292–296.
[38] E.A. Konstantinova, A.I. Kokorin, S. Saktivel, H. Kisch, K. Lips, Chimia 61 (2007) 810–814.
[39] M.S. Wong, S.W. Hsu, K.K. Rao, C.P. Kumar, J. Mol. Catal. A 279 (2008) 20–26.
[40] J.H. Park, S. Kim, A.J. Bard, Nano Lett. 6 (2006) 24–28.
[41] X. Yang, C. Cao, L. Erickson, K. Hohn, R. Maghirang, K. Klabunde, J. Catal. 260 (2008) 128–133.
[42] V. Trevisan, E. Ghedini, M. Signoretto, F. Pinna, C.L. Bianchi, Microchem. J. 112 (2014) 186–189.
[43] S. Brunauer, P.H. Emmett, E. Teller, J. Am. Chem. Soc. 60 (1938) 309–319.
[44] E.P. Barrett, L.G. Joyner, P.P. Halenda, J. Am. Chem. Soc. 73 (1951) 373–380.
[45] M. Signoretto, E. Ghedini, V. Trevisan, C.L. Bianchi, M. Ongaro, G. Cruciani, Appl. Catal. B: Environ. 95 (2010) 130–136.
[46] M.J. Illán-Gómez, A. Bueno-López, J.R. González-Velasco, Appl. Catal. B: Environ. 147 (2014) 420–428.
[47] G. Husken, M. Hunger, H.J.H. Brouwers, Build. Environ. 44 (2009) 2463–2474.
[48] B.N. Shelimov, N.N. Tolkachev, O.P. Tkachenko, G.N. Baeve, K.V. Klementiev, A.Y. Stakheev, V.B. Kazansky, J. Photochem. Photobiol. A 195 (2008) 81–88.
[49] ISO 22197-1:2007, 'Fine Ceramics, Advanced Technical Ceramics – Test Method for Air-Purification Performance of Semiconducting Photocatalytic Materials – Part 1: Removal of Nitric Oxide', ISO, Geneva, 2007.
[50] K. Zhang, X. Wang, T. He, X. Guo, Y. Feng, Powder Technol. 253 (2014) 608–613.
[51] M.V. Dozzi, E. Selli, J. Photochem. Photobiol. C 14 (2013) 13–28.
[52] X. Chen, C. Burda, J. Am. Chem. Soc. 130 (2008) 5018–5019.
[53] H. Irie, S. Washizuka, K. Hashimoto, Thin Solid Films 510 (2006) 21–25.
[54] W. Ren, Z. Ai, F. Jia, L. Zhang, X. Fan, Z. Zou, Appl. Catal. B: Environ. 69 (2007) 138–144.
[55] Y.Z. Li, D.S. Hwang, N.H. Lee, S.J. Kim, Chem. Phys. Lett. 404 (2005) 25–29.
[56] Y. Ao, J. Xu, D. Fu, C. Yuan, Microporous. Mesoporous. Mater. 118 (2009) 382–386.
[57] S. Li, J. Yu, W. Wang, Phys. Chem. Chem. Phys. 12 (2010) 12308–12315.
[58] C. Chen, W. Ma, J. Zhao, Curr. Org. Chem. 14 (2010) 630–644.
[59] W.J. Yin, H. Tang, S.H. Wei, M.M. Al-Jassim, J. Turner, Y. Yan, Phys. Rev. B 82 (2010) 045106.
[60] X. Ma, Y. Wu, Y. Lu, J. Xu, Y. Wang, Y. Zhu, J. Phys. Chem. C 115 (2011) 16963–16969.